J|A|C|S
ARTICLES
Published on Web 05/22/2007

Cyclotetraphosphinophosphonium Ions: Synthesis, Structures, and Pseudorotation

C. Adam Dyker,[†] Susanne D. Riegel,[†] Neil Burford,*[,†] Michael D. Lumsden,[‡] and Andreas Decken[§]

Contribution from the Department of Chemistry and Atlantic Region Magnetic Resonance Center, Dalhousie University, Halifax, Nova Scotia, B3H 4J3, Canada, and Department of Chemistry, University of New Brunswick, Fredericton, New Brunswick, E3A 6E2, Canada

Received February 2, 2007; E-mail: neil.burford@dal.ca

Abstract: The first derivatives of catenated cyclotetraphosphinophosphonium cations, $[(PhP)_4PPhMe]^+$ (**8a**), $[(MeP)_4PMe_2]^+$ (**8b**), $[(CyP)_4PPh_2]^+$ (**8d**), $[(CyP)_4PMe_2]^+$ (**8e**), $[(PhP)_4PPh_2]^+$ (**8f**), $[(PhP)_4PMe_2]^+$ (**8g**), are synthesized as trifluoromethanesulfonate (triflate, $OSO_2CF_3^-$) salts through the reaction of cyclopentaphosphines $(PhP)_5$ (**4a**) or $(MeP)_5$ (**4b**) with methyl triflate (MeOTf) or by a net phosphenium ion [PR_2^+, R = Ph, Me; from R_2PCl and trimethylsilyltriflate (Me_3SiOTf)] insertion into the P−P bond of either cyclotetraphosphine $(CyP)_4$ (**3c**) or cyclopentaphosphines $(PhP)_5$ (**4a**) or $(MeP)_5$ (**4b**). Although more conveniently prepared from **4a**, compound **8a**[OTf] can also be formed from $(PhP)_4$ (**3a**) and MeOTf, and derivatives **8f**[OTf] and **8g**[OTf] are also accessible through reactions of **3a** and R_2PCl/Me_3SiOTf with R = Ph or Me, respectively. A tetrachlorogallate salt of $[(PhP)_4PPh^tBu]^+$ (**8c**) has been synthesized by alkylation of **4a** with ^{t}BuCl/$GaCl_3$. $^{31}P\{^1H\}$ NMR parameters for all derivatives of **8** have been determined by iterative simulation of experimental data. Derivatives **8a**[OTf], **8b**[OTf], **8c**[$GaCl_4$], **8e**[OTf], **8f**[OTf], and **8g**[OTf] and have been characterized by X-ray crystallography, showing the most favorable all-*trans* configuration of substituents for the phosphine centers, thus minimizing steric interactions. Each derivative adopts a unique envelope or twist conformation of C_1 symmetry. The effective C_2 symmetry observed for **8b**, **d**, **e**, **f**, and **g** in solution, signified by their $^{31}P\{^1H\}$ NMR AA′BB′X spin systems, implies a rapid conformational exchange for derivatives of **8**. The core frameworks of the cations in the solid state are viewed as snapshots of different conformational isomers within the solution-phase pseudorotation process.

Introduction

Analogies between the chemistry of carbon and phosphorus are often rationalized in terms of their similar electronegativities, and frequent reference is made to their diagonal relationship in the Periodic Table.[1] In this context, homoatomic bonding, which is responsible for the extent of organic chemistry, promises a diverse and extensive *catena*-phosphorus chemistry that has not yet been fully realized. New versatile synthetic methods have enabled the discovery of *catena*-phosphonium ions[2−9] that complement the well-known series of *catena*-phosphines,[10−13] new borane complexes of *catena*-phosphines,[14] and *catena*-phosphorus anions,[10−12,15−23] each featuring phosphorus centers as isolobal analogues of tetrahedral carbon environments. The phosphinophosphonium frameworks **5**,[2,3,5] **6**,[7] and **7**[7] (Scheme 1) derive from the neutral polyphosphines **1**, **2**, and **3** but have been prepared from a variety of starting materials that provide guidelines for the development of larger frameworks. We now report the synthesis and characterization of racemic cyclotet-

[†] Department of Chemistry, Dalhousie University.
[‡] Atlantic Region Magnetic Resonance Center, Dalhousie University.
[§] Department of Chemistry, University of New Brunswick.

(1) Dillon, K. B.; Mathey, F.; Nixon, J. F. *Phosphorus: The Carbon Copy*; John Wiley & Sons: New York, 1997.
(2) Burford, N.; Cameron, T. S.; Ragogna, P. J.; Ocando-Mavarez, E.; Gee, M.; McDonald, R.; Wasylishen, R. E. *J. Am. Chem. Soc.* **2001**, *123*, 7947−7948.
(3) Burford, N.; Ragogna, P. J.; McDonald, R.; Ferguson, M. *J. Am. Chem. Soc.* **2003**, *125*, 14404−14410.
(4) Burford, N.; Ragogna, P. J. *Dalton Trans.* **2002**, 4307−4315.
(5) Burford, N.; Ragogna, P. J.; McDonald, R.; Ferguson, M. J. *Chem. Commun.* **2003**, 2066−2067.
(6) Burford, N.; Dyker, C. A.; Decken, A. *Angew. Chem., Int. Ed.* **2005**, *44*, 2364−2367.
(7) Burford, N.; Dyker, C. A.; Lumsden, M. D.; Decken, A. *Angew. Chem., Int. Ed.* **2005**, *44*, 6196−6199.
(8) Weigand, J. J.; Burford, N.; Lumsden, M. D.; Decken, A. *Angew. Chem., Int. Ed.* **2006**, *45*, 6733−6737.
(9) Dyker, C. A.; Burford, N.; Lumsden, M. D.; Decken, A. *J. Am. Chem. Soc.* **2006**, *128*, 9632−9633.
(10) Baudler, M. *Angew. Chem., Int. Ed.* **1982**, *21*, 492−512.
(11) Baudler, M. *Angew. Chem., Int. Ed.* **1987**, *26*, 419−441.
(12) Baudler, M.; Glinka, K. *Chem. Rev.* **1993**, *93*, 1623−1667.
(13) Baudler, M.; Glinka, K. *Chem. Rev.* **1994**, *94*, 1273−1297.
(14) Wolf, R.; Finger, M.; Limburg, C.; Willis, A. C.; Wild, S. B.; Hey-Hawkins, E. *Dalton Trans.* **2006**, 831−837.
(15) von Schnering, H. G.; Hönle, W. *Chem. Rev.* **1988**, *88*, 243−273.
(16) Geier, J.; Harmer, J.; Grutzmacher, H. *Angew. Chem., Int. Ed.* **2004**, *43*, 4093−4097.
(17) Geier, J.; Ruegger, H.; Worle, M.; Grutzmacher, H. *Angew. Chem., Int. Ed.* **2003**, *42*, 3951−3954.
(18) Schisler, A.; Lonnecke, P.; Gelbrich, T.; Hey-Hawkins, E. *Dalton Trans.* **2004**, 2895−2898.
(19) Wolf, R.; Schisler, A.; Lonnecke, P.; Jones, C.; Hey-Hawkins, E. *Eur. J. Inorg. Chem.* **2004**, 3277−3286.
(20) Lerner, H.-W.; Margraf, G.; Kaufmann, L.; Bats, J. W.; Bolte, M.; Wagner, M. *Eur. J. Inorg. Chem.* **2005**, 1932−1939.
(21) Lerner, H.-W.; Bolte, M.; Karaghiosoff, K.; Wagner, M. *Organometallics* **2004**, *23*, 6073−6076.
(22) Stein, D.; Dransfeld, A.; Flock, M.; Riiegger, H.; Grutzmacher, H. *Eur. J. Inorg. Chem.* **2006**, 4157−4167.
(23) Wolf, R.; Hey-Hawkins, E. *Z. Anorg. Allg. Chem.* **2006**, *632*, 727−734.

10.1021/ja070764f CCC: $37.00

Scheme 1

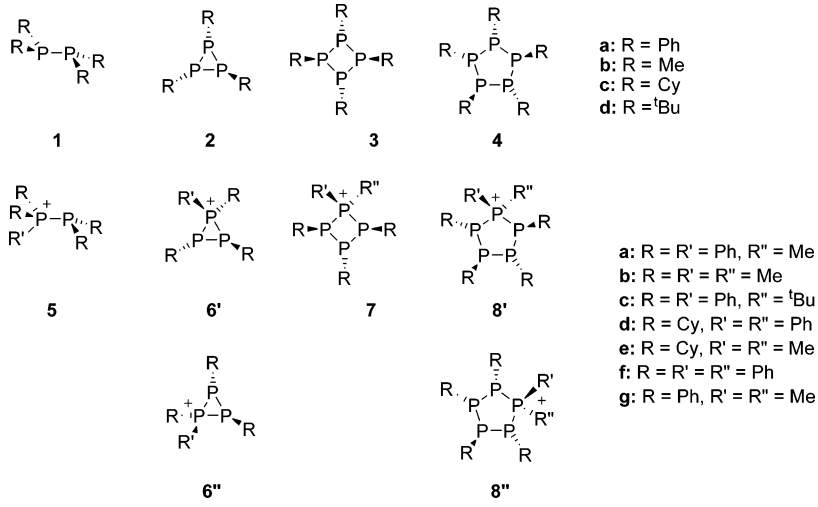

Table 1. Crystallographic Data for **8b**[OTf], **8c**[$GaCl_4$], **8e**[OTf], **8f**[OTf], and **8g**[OTf]

compound	$[(MeP)_4PMe_2]$ [OTf]	$[(PhP)_4PPh(^tBu)]$ $[GaCl_4]$	$[(CyP)_4PMe_2]$ [OTf]	$[(PhP)_4PPh_2]$ [OTf][6]	$[(PhP)_4PMe_2]$ [OTf]
label	**8b**[OTf]	**8c**[$GaCl_4$]	**8e**[OTf]	**8f**[OTf]	**8g**[OTf]
CCDC number	632891	632888	632889	257691	632890
formula	$C_7H_{18}F_3O_3P_5S$	$C_{34}H_{34}Cl_4GaP_5$	$C_{27}H_{50}F_3O_3P_5S$	$C_{37}H_{30}F_3O_3P_5S$	$C_{27}H_{26}F_3O_3P_5S$
molecular weight (g/mol)	394.12	808.98	666.58	766.52	642.39
crystal system	orthorhombic	triclinic	monoclinic	monoclinic	triclinic
space group	$P2_12_12_1$	$P\bar{1}$	$P2_1/c$	$P2_1/c$	$P\bar{1}$
color	colorless	colorless	colorless	colorless	colorless
a /Å	11.5785(7)	10.2161(12)	20.098(2)	10.6004(6)	9.947(1)
b /Å	12.1458(7)	11.7132(14)	34.842(3)	16.7110(8)	12.758(2)
c /Å	24.547(1)	16.928(2)	9.6712(7)	20.061(1)	12.954(2)
α /deg	90	82.232(2)	90	90	109.358(2)
β /deg	90	80.760(2)	94.697(1)	92.255(1)	97.345(2)
γ /deg	90	66.707(2)	90	90	104.076(2)°
V/Å^3	3452.0(3)	1830.7(4)	6749.7(9)	3550.8(3)	1464.8(3)
T /K	193(1)	198(1)	213(1)	198(1)	198(1)
Z	8	2	8	4	2
R^a ($I > 2\sigma(I)$, all data)	0.0412, 0.0538	0.0329, 0.0486	0.0528, 0.0848	0.0343, 0.0502	0.0364, 0.0581
$wR_2{}^b$ ($I > 2\sigma(I)$, all data)	0.1018, 0.1104	0.0774, 0.0893	0.1306, 0.1389	0.0861, 0.0930	0.0620, 0.0647
GOF[c]	1.061	1.060	1.079	1.053	0.832
$\Delta\rho$ max and min /e Å^{-3}	+0.813, −0.336	+0.720, −0.403	+0.997, −0.416	+0.432, −0.421	+0.533, −0.49a

[a] $R = \sum|F_o| - |F_c|/\sum|F_o|$. [b] $wR_2 = (\sum[w(F_o^2 - F_c^2)^2]/\sum[w(F_o^4])^{1/2}$. [c] GOF $= [\sum w(F_o^2 - F_c^2)/(n - p)]^{1/2}$, where n = number of reflections, and p = number of parameters.

raphosphinophosphonium salts (**8′** and **8″**)[6] as the next member of the series of cyclo-*catena*-phosphorus monocations. Although salts of framework **8** were proposed on the basis of elemental analysis data,[24,25] the first structural and spectroscopic characterization are presented here for a number of derivatives, together with assessments of conformational features.

Experimental Section

Reactions were carried out in a glove box under an inert N_2 atmosphere. Solvents were dried on an MBraun solvent purification system and stored over molecular sieves prior to use. $(P^tBu)_4$,[26] $(PCy)_4$,[27] $(PhP)_4$,[28] $(PPh)_5$,[27] and $(PMe)_5$[26] were prepared according to literature methods. Me_2PCl and MeOTf were purchased from Strem and Aldrich, respectively, and were used as received. Ph_2PCl and Me_3SiOTf were purchased from Aldrich and were purified by vacuum distillation prior to use.

Solution ^1H, ^{13}C, and ^{31}P NMR spectra were collected at room temperature on Bruker AC-250 and Bruker Avance 500 NMR spectrometers. Chemical shifts are reported in ppm relative to an external reference standard [100% $SiMe_4$ (^1H, ^{13}C), and 85% H_3PO_4 (^{31}P)]. NMR spectra of reaction mixtures were obtained by transferring an aliquot of the bulk solution to a 5 mm NMR tube. These tubes were flame sealed or capped and sealed with Parafilm. All reported $^{31}P\{^1H\}$ NMR parameters were derived by computer simulation using gNMR[29] at fields of 101.3 and 202.6 MHz. The signs of the P−P coupling constants reported in Tables 3 and 4 have been established by assuming that the sign of one bond P(III)−P(III) coupling constants is negative.[30]

Infrared spectra were collected on samples prepared as Nujol mulls between CsI plates using a Bruker Vector FT-IR spectrometer. Peaks are reported in wavenumbers (cm^{-1}) with ranked intensities in parentheses, where a value of one corresponds to the most intense peak in the spectrum. Melting points were obtained on samples sealed in glass capillaries under dry nitrogen using an Electrothermal apparatus. Chemical analyses were performed on selected compounds by Canadian Microanalytical Services Ltd., Delta, British Columbia, Canada.

(24) Issleib, K.; Rockstroh, C.; Duchek, I.; Fluck, E. *Z. Anorg. Allg. Chem.* **1968**, *360*, 77−87.
(25) Appel, R.; Milker, R. *Z. Anorg. Allg. Chem.* **1975**, *417*, 161−170.
(26) Baudler, M.; Glinka, K. *Inorg. Synth.* **1989**, *25*, 1−5.
(27) Henderson, W. A.; Epstein, M.; Seichter, F. S. *J. Am. Chem. Soc.* **1963**, *85*, 2462−2466.
(28) Breen, T. L.; Stephan, D. W. *Organometallics* **1997**, *16*, 365−369.
(29) Budzelaar, P. H. M. *gNMR for Windows. (4.0)*; Cherwell Scientific Publishing Limited: Oxford, 1997.
(30) Forgeron, M. A. M.; Gee, M.; Wasylishen, R. E. *J. Phys. Chem.* **2004**, *108*, 4895−4908.

Scheme 2

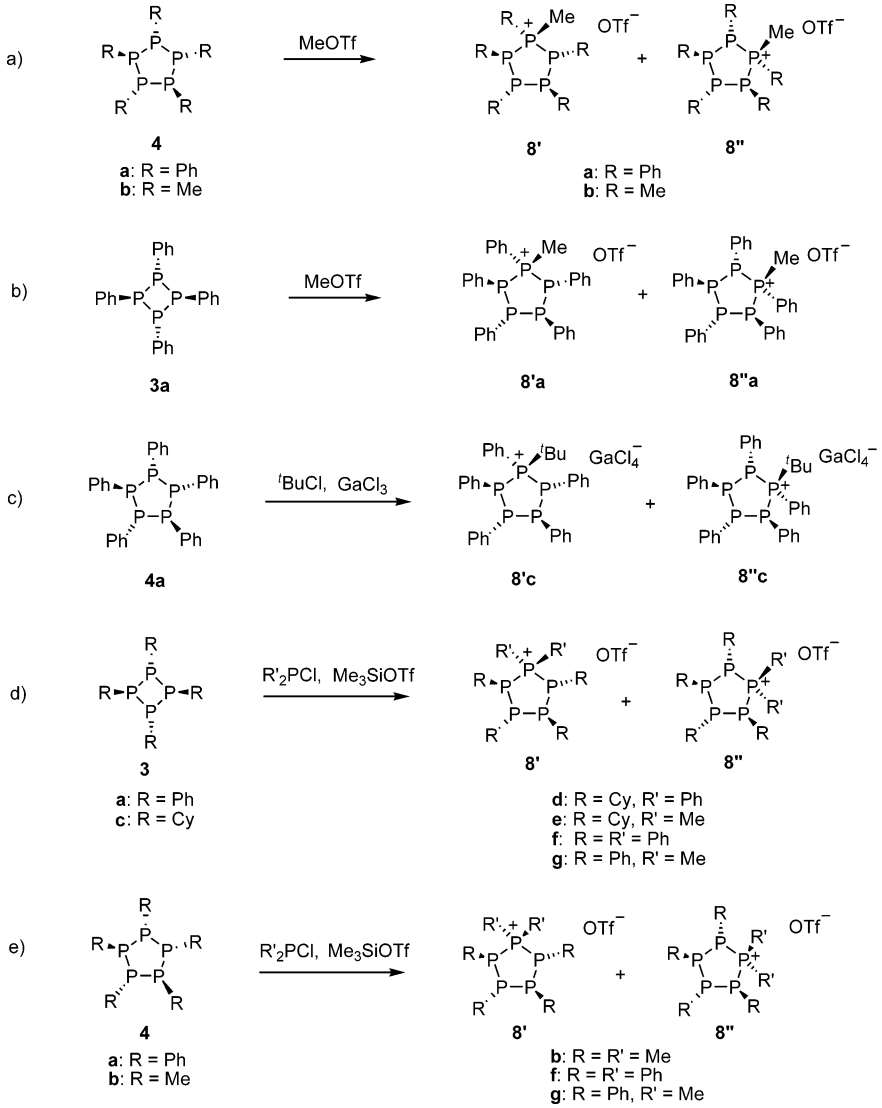

Unless otherwise stated, crystals for single-crystal X-ray diffraction studies were obtained by vapor diffusion at RT, which involved dissolving a sample (0.05−0.10 g) in a minimal amount (1−2 mL) of a polar solvent (CH_2Cl_2, $CHCl_3$, fluorobenzene) in a 5 mL vial placed within a capped 20 mL vial containing ∼5 mL of a less polar solvent (Et_2O, hexane). After deposition of crystals, the solvent was carefully removed using a pipet and the crystals were coated with Paratone oil. Single-crystal X-ray diffraction data were collected using a Bruker AXS P4/SMART 1000 diffractometer. All measurements were made with graphite monochromated Mo Kα radiation. The data were reduced (SAINT)[31] and corrected for absorption (SADABS)[32] and were corrected for Lorentz and polarization effects. The structures were solved by direct methods and expanded using Fourier techniques. Full matrix least-squares refinement was carried out on F^2 data using the program SHELX97.[33] Non-hydrogen atoms were refined anisotropically. Hydrogen atoms were included in geometrically calculated positions, and refined using a riding model, except for **8f**[OTf] for which hydrogen atoms were found in Fourier difference maps and refined anisotropically. The crystal of **8g**[OTf] was a twin and the two orientation matrices for two components was determined (RLATT, GEMINI).[34,35] Refinement details are summarized in Table 1. The full set of crystallographic results has been deposited with CCDC and reference numbers are given in Table 1.

[(PhP)$_4$PPhMe][OTf], 8a[OTf].[6] MeOTf (0.038 mL, 0.33 mmol) was added to a solution of $(PhP)_5$ (0.100 g, 0.19 mmol) in benzene (3 mL). After stirring for 5 min, hexane (2 mL) was added to yield an oily precipitate, which was left at room temperature to settle overnight. The solvents were decanted from the precipitate, which was then crystallized as **8a**[OTf]·1.5 C_6H_6 over 24 h by vapor diffusion of Et_2O into a $CHCl_3$ solution at room temperature; Yield: 0.107 g (0.139 mmol, 73% for **8a**[OTf]·1.5 C_6H_6 at least, noting solvated benzene is partially removed *in vacuo*); Dp 97−107 °C; $^{31}P\{^1H\}$ NMR (101.3 MHz, $CDCl_3$, 298 K): ABCDX spin system; $\delta A = -35.7$ ppm, $\delta B = -33.7$ ppm, $\delta C = -31.8$ ppm, $\delta D = -24.6$ ppm, $\delta X = 22.2$ ppm, $^1J_{AB} = -162$ Hz, $^1J_{AX} = -328$ Hz, $^1J_{BC} = -166$ Hz, $^1J_{CD} = -193$ Hz, $^1J_{DX} = -315$ Hz, $^2J_{AC} = 71$ Hz, $^2J_{AD} = -14$ Hz, $^2J_{BD} = 58$ Hz, $^2J_{BX} = 30$ Hz, $^2J_{CX} = 17$ Hz; ^{1}H NMR (500.1 MHz, $CDCl_3$, 298 K): $\delta = 7.96$ ppm ($^3J_{HH} = 7$ Hz, $^3J_{HH} = 7$ Hz, 2H), 7.88 ppm (m, 2H), 7.72 ppm (m, 2H), 7.60−7.40 ppm (m, 17H), 7.29 ppm (m, 2H), 2.23 ppm (dd, $J_{PH} = 12$ Hz, $J_{PH} = 7.5$ Hz, 3H); ^{13}C NMR (125.8 MHz, DEPTQ135, $CDCl_3$, 298 K): $\delta = 135.5$ (m, +), 134.9 (m, +), 134.4−133.8 (m, +), 132.9 (m, +), 131.9 (s, +), 131.5 (s, +), 131.3 (s, +), 130.4 (m, +), 130.0 (s, +), 129.9 (s, +), 129.8 (s, +), 129.7 (m, +), 9.4 ppm (m, +); FT-

(31) *SAINT 6.02*; Bruker AXS, Inc.: Madison, WI, 1997−1999.
(32) Sheldrick, G. *SADABS*; Bruker AXS, Inc.: Madison, WI, 1999.
(33) Sheldrick, G. M. *SHELXL-97, Program for Crystal Structure Determination*; University of Goettingen: Germany, 1997.
(34) RLATT 2.72; Bruker AXS, Inc.: Madison, WI, 1999.
(35) GEMINI 1.0; Bruker AXS, Inc.: Madison, WI, 1999.

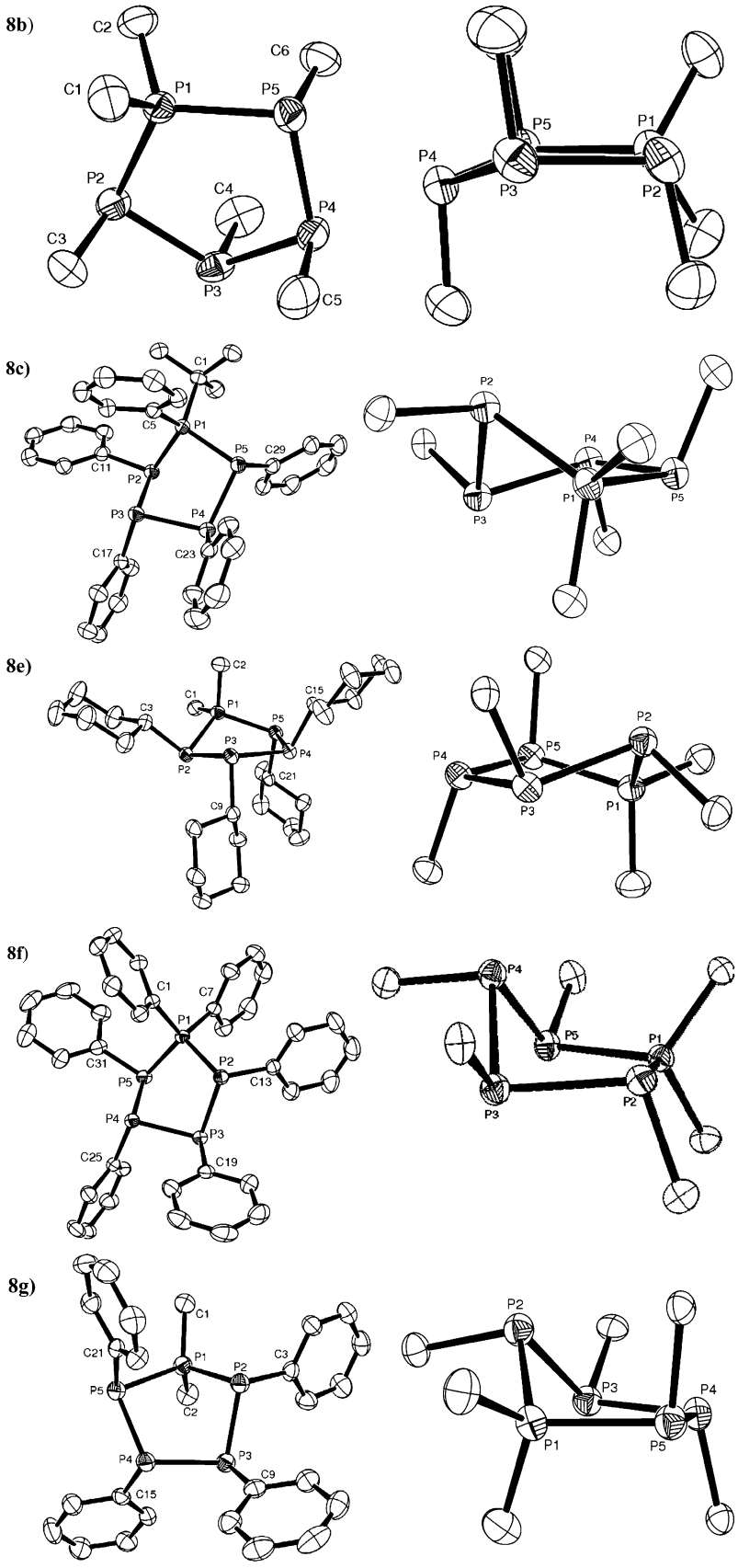

Figure 1. (Left) Solid-state structure of the *R, S, S, R* enantiomer of the cation in **8b**[OTf], **8c**[$GaCl_4$], **8e**[OTf], **8f**[OTf], and **8g**[OTf] (hydrogen atoms omitted). (Right) In-plane view of the phosphorus framework and α-carbon centers for each cation. Tetracoordinate phosphorus centers are designated P1. Thermal ellipsoids are shown at the 50% probability level.

IR (nujol, ranked intensities): 1261(1), 1219(8), 1146(7), 1029(6), 996-(12), 903(13), 805(9), 752(4), 740(5), 689(2), 635(3), 570(11), 515(10), 456(14) cm^{-1}; $^{31}P\{^1H\}$ NMR spectra of reaction mixtures show that **8a**[OTf] is the exclusive product from the addition of MeOTf (0.007 mL, 0.064 mmol) to $(PhP)_4$ (0.014 g, 0.032 mmol) in CH_2Cl_2 (1 mL).

[(MeP)$_4$PMe$_2$][OTf], 8b[OTf]. MeOTf (0.051 mL, 0.45 mmol) was added dropwise to solution of $(PMe)_5$ (0.086 g, 0.37 mmol) in CH_2Cl_2 (3 mL). After stirring for 30 min, Et_2O (~5 mL) was added to precipitate a white powder. The solvents were decanted and the precipitate was washed with Et_2O (2 × 2 mL). **8b**[OTf] was recrystallized by vapor diffusion of Et_2O into a solution of CH_2Cl_2 at room temperature. Yield: 0.094 g (0.24 mmol, 77%); elemental analysis (%) calcd for $C_7H_{18}F_3O_3P_5S$: C 21.33, H 4.60; found: C 20.32, H 4.69.

8b[OTf] is also formed from the dropwise addition of a CH_2Cl_2 (2 mL) solution of Me_2PCl (21.9 μL, 0.28 mmol) and Me_3SiOTf (60.3 μL, 0.33 mmol) to a CH_2Cl_2 (2 mL) solution of $(PMe)_5$ (0.042 g, 0.19 mmol). The resultant solution was allowed to stir for 30 min before Et_2O (6 mL) was added, affording white precipitate of **8b**[OTf]. The solvents were decanted and the precipitate was washed with Et_2O (2 × 2 mL). Yield: 0.052 g (0.13 mmol, 71%).

Mp 109−112 °C; $^{31}P\{^1H\}$ NMR (101.3 MHz, CH_2Cl_2, 298 K): AA′BB′X spin system; $\delta A = 20$ ppm, $\delta B = 24$ ppm, $\delta X = 101$ ppm, $^1J_{BB'} = -263$ Hz, $^1J_{AB} = {}^1J_{A'B'} = -277$ Hz, $^1J_{AX} = {}^1J_{A'X} = -346$, $^2J_{BX} = {}^2J_{B'X} = -3$ Hz, $^2J_{AB'} = {}^2J_{A'B} = 16$ Hz, $^2J_{AA'} = -19$ Hz; FT-IR (nujol, ranked intensities): 1377(5), 1253(1), 1157(2), 1027(3), 965-(6), 930(7), 870(8), 756(10), 697(11), 637(4), 572(12), 516(9) cm^{-1}.

$^{31}P\{^1H\}$ NMR spectra of crystalline samples redissolved show the presence of other isomers of **8b**[OTf] that could not be unequivocally identified.

[(PhP)$_4$PPh^{t}Bu)][GaCl$_4$], 8c[GaCl$_4$]. $GaCl_3$ (0.034 g, 0.19 mmol) was added directly to a benzene solution (2 mL) of $(PPh)_5$ (0.104 g, 0.19 mmol) giving a broad signal in $^{31}P\{^1H\}$ NMR spectrum assigned to the adduct $(PPh)_5 \cdot GaCl_3$. ^{t}BuCl (20.9 μL, 0.19 mmol) was added dropwise, resulting in the formation of a yellow oily layer. After stirring for 30 min, Et_2O (~5 mL) was added. The resultant thick oil was washed with Et_2O (2 × 2 mL) and dissolved in MeCN. Bright-yellow crystals settled out of this solution after ~30 min. Yield: 0.123 g (0.15 mmol, 81%); Mp 161−166 °C; $^{31}P\{^1H\}$ NMR (101.3 MHz, d_3-MeCN, 298 K): ABCDX spin system; $\delta A = -45.9$ ppm, $\delta B = -38.4$ ppm, δC −31.1 ppm, $\delta D = -28.5$ ppm, $\delta X = 26.5$ ppm, $^1J_{AB} = -178$ Hz, $^1J_{AD} = -137$ Hz, $^1J_{BC} = -229$ Hz, $^1J_{CX} = -350$ Hz, $^1J_{DX} = -404$ Hz, $^2J_{AC} = 4$ Hz, $^2J_{AX} = 38$ Hz, $^2J_{BD} = 66$ Hz, $^2J_{BX} = 6$ Hz, $^2J_{CD} = -19$ Hz; $^1H\{^{31}P\}$ NMR (500.1 MHz, d_3-MeCN, 298 K): $\delta = 8.21$ ppm (d, 2H, $^3J_{HH} = 10$ Hz), 8.06 ppm (d, 1H, $^3J_{HH} = 9$ Hz), 7.96 ppm (d, 2H, $^3J_{HH} = 9$ Hz), 7.78−7.34 ppm (m, 20H), 1.14 ppm (s, 9H); ^{13}C NMR data could not be obtained for **8c** as it decomposes in solution within an hour yielding a number of unidentifiable products; FT-IR (nujol, ranked intensities): 1581(7), 1513(14), 1434(11), 1304(13), 1261(6), 1168(8), 1081(9), 1020(2), 998(10), 800(5), 741(1), 690(3), 479(4), 470(12) cm^{-1}.

[(CyP)$_4$PPh$_2$][OTf], 8d[OTf]. Me_3SiOTf (0.074 mL, 0.41 mmol) was added to a solution of Ph_2PCl (0.066 mL, 0.37 mmol) in CH_2Cl_2 (2 mL). The resultant solution was added to a mixture of $(PCy)_4$ (0.084 g, 0.18 mmol) in CH_2Cl_2 (2 mL). After vigorous stirring for 20 min, the $^{31}P\{^1H\}$ NMR spectrum of the solution showed **8d**[OTf] as the major product. $^{31}P\{^1H\}$ NMR (101.3 MHz, CH_2Cl_2, 298 K): AA′BB′X spin system; $\delta A = -15$ ppm, $\delta B = -2$ ppm, $\delta X = 52$ ppm, $^1J_{AA'} = -247$ Hz, $^1J_{AB} = {}^1J_{A'B'} = -262$ Hz, $^1J_{BX} = {}^1J_{B'X} = -352$ Hz, $^2J_{AX} = {}^2J_{A'X} = 2$ Hz, $^2J_{AB'} = {}^2J_{A'B} = 0$ Hz, $^2J_{BB'} = -21$ Hz. Excess Ph_2PCl (82 ppm) and three minor products were observed; one observed as an AB_2X spin system ($\delta A = -54$ ppm, $\delta B = -44$ ppm, $\delta X = -2$ ppm, $^1J_{AB} = -123$ Hz, $^1J_{BX} = -233$ Hz, $^2J_{AX} = 14$ Hz**)** assigned to $[(CyP)_3PPh_2][OTf]$, one assigned to $[Ph_2P-PPh_2-PPh_2][OTf]$,[6] and an unassigned peak at 46 ppm.

[(CyP)$_4$PMe$_2$][OTf], 8e[OTf]. Me_3SiOTf (0.075 mL, 0.42 mmol) was added to a solution of Me_2PCl (0.026 mL, 0.33 mmol) in CH_2Cl_2 (3 mL). This solution was then added to a mixture of $(PCy)_4$ (0.126 g, 0.28 mmol) in CH_2Cl_2 (3 mL) and stirred for 4 days. After filtration and removal of volatiles *in vacuo*, the white solid was washed with hexane (2 × 3 mL). Slow diffusion of hexane vapor into a fluorobenzene solution of the white solid at room temperature afforded crystals of **8e**[OTf]. Yield: 0.048 g (0.072 mmol, 26%); Mp 159−161 °C; $^{31}P\{^1H\}$ NMR (101.3 MHz, $CDCl_3$, 298 K): AA′BB′X spin system; $\delta A = -14$ ppm, $\delta B = -8$ ppm, $\delta X = 42$ ppm, $^1J_{AA'} = -255$ Hz, $^1J_{AB} = {}^1J_{A'B'} = -264$ Hz, $^1J_{BX} = {}^1J_{B'X} = -332$ Hz, $^2J_{AX} = {}^2J_{A'X} = 9$ Hz, $^2J_{AB'} = {}^2J_{A'B} = 0$ Hz, $^2J_{BB'} = -21$ Hz; ^1H NMR (500.1 MHz, $CDCl_3$, 298 K): 2.35 ppm (m, 8H), 2.15 ppm (m, 2H), 2.00 ppm (m, 6H), 1.87 ppm (m, 10H), 1.75 ppm (m, 4H), 1.46 ppm (m, 8H), 1.30 ppm (m, 12H); ^{13}C NMR (125.8 MHz, DEPTQ135,$CDCl_3$, 298 K): 36.3 ppm (m, +), 34.5 ppm (m, +), 33.6 ppm (m, −), 33.0 ppm (m, −), 32.5 ppm (m, −), 32.2 ppm (m, −), 27.0 ppm (m, −), 26.8 ppm (m, −), 26.5 ppm (m, −), 25.6 ppm (s, −), 25.3 ppm (s, −), 12.8 ppm (m, +); FT-IR (nujol, ranked intensities): ν = 1309(11), 1256(1), 1220(5), 1147(4), 1031(3), 958(8), 906(9), 803(10), 635(2), 571(7), 516(6) cm^{-1}.

[(PhP)$_4$PPh$_2$][OTf], 8f[OTf][6]. Ph_2PCl (0.045 mL, 0.25 mmol) was added to Me_3SiOTf (0.060 mL, 0.30 mmol) in CH_2Cl_2 (2 mL) followed by the addition of a CH_2Cl_2 (2 mL) solution of $(PhP)_5$ (0.100 g, 0.185 mmol). The solvent was removed *in vacuo* and the solid washed with hexane (2 × 4 mL). Yield: 0.123 g (0.16 mmol, 87%); Dp 65−75 °C; Elemental analysis (%) calcd for $C_{37}H_{30}F_3O_3P_5S$: C 58.0, H 3.9, P 20.2; found: C 57.4, H 3.9, P 20.4; $^{31}P\{^1H\}$ NMR (101.3 MHz, $CDCl_3$, 298 K): AA′BB′X spin system; $\delta A = -42$ ppm, $\delta B = -36$ ppm, $\delta X =$ 22 ppm, $^1J_{AA'} = -142$ Hz, $^1J_{AB} = {}^1J_{A'B'} = -160$ Hz, $^1J_{BX} = {}^1J_{B'X} = -325$ Hz, $^2J_{AX} = {}^2J_{A'X} = 28$ Hz, $^2J_{AB'} = {}^2J_{A'B} = 79$ Hz, $^2J_{BB'} = -14$ Hz; ^1H NMR (500.1 MHz, $CDCl_3$, 298 K): $\delta = 7.92$ ppm (m, 4H), 7.69 ppm (m, 2H), 7.47 ppm (m, 16H), 7.28 ppm (m, 8H); ^{13}C NMR (125.8 MHz, DEPTQ135, $CDCl_3$, 298 K): $\delta = 135.9$ ppm (m, +), 135.0 ppm (s, +), 134.1 ppm (m, +), 132.5 ppm (s, +), 131.7 ppm (s, +), 130.2 ppm (s, +), 130.0 ppm (s, +), 129.9 ppm (m, +); FT-IR (nujol, ranked intensities): 1312(11), 1263(1), 1146(6), 1093(8), 1029-(2), 997(9), 843(7), 740(3), 687(5), 635(4), 570(12), 517(10) cm^{-1}. Crystals for X-ray diffraction were obtained by vapor diffusion of Et_2O into a CH_2Cl_2 solution at −25 °C; $^{31}P\{^1H\}$ NMR spectra of reaction mixtures show that **8f**[OTf] is the exclusive product from the addition of a solution of Ph_2PCl (0.019 mL, 0.106 mmol) and Me_3SiOTf (0.023 mL, 0.127 mmol) in CH_2Cl_2 (3 mL) to solid $(PhP)_4$ (0.045 g, 0.104 mmol).

[(PhP)$_4$PMe$_2$][OTf], 8g[OTf][6]. Me_2PCl (0.014 mL, 0.185 mmol) was added to Me_3SiOTf (0.040 mL, 0.22 mmol) in CH_2Cl_2 (2 mL). This solution was added dropwise to $(PhP)_5$ (0.050 g, 0.093 mmol) in CH_2Cl_2 (2 mL). Filtration, followed by slow diffusion of Et_2O vapor into the solution at −25 °C, gave a precipitate of **8g**[OTf]. Yield: 0.027 g (0.042 mmol, 45%); Dp 142−145 °C. Elemental analysis (%) calcd for $C_{27}H_{26}F_3O_3P_5S$: C 50.5, H 4.1; found: C 49.4, H 3.6; $^{31}P\{^1H\}$ NMR (101.3 MHz, $CDCl_3$, 298 K): AA′BB′X spin system; $\delta A = -32$ ppm, $\delta B = -26$ ppm, $\delta X = 27$ ppm, $^1J_{BB'} = -186$ Hz, $^1J_{AB} = {}^1J_{A'B'} = -192$ Hz, $^1J_{AX} = {}^1J_{A'X} = -315$ Hz, $^2J_{BX} = {}^2J_{B'X} = 24$ Hz, $^2J_{AB'} = {}^2J_{A'B} = 50$ Hz, $^2J_{AA'} = -15$ Hz; ^1H NMR (500.1 MHz, $CDCl_3$, 298 K): $\delta = 7.86$ ppm (m, 8H), 7.63 ppm (m, 2H) 7.55 ppm (m, 4H), 7.49 ppm (m, 6H), 1.86 ppm (m, 6H); ^{13}C NMR (125.8 MHz, DEPTQ135, $CDCl_3$, 298 K): $\delta = 135.3$ ppm (m, +), 133.8 ppm (m, +), 132.5 ppm (s, +), 131.1 ppm (s, +), 130.3 ppm (s, +), 129.8 ppm (s, +), 10.4 ppm (m, +); FT-IR (nujol, ranked intensities): 1304(8), 1288(1), 1247(2), 1150(7), 1032(3), 958(10), 918(9), 733(4), 691(5), 638(6), 572(13), 516(12), 465(11) cm^{-1}. Crystals suitable for X-ray diffraction were obtained from the addition of Et_2O (~1.5 mL) to a solution of 0.26 g of **8g**[OTf] in CH_2Cl_2 (~1.5 mL) and letting it stand at room temperature for 5 days (Yield: 0.19 g; $^{31}P\{^1H\}$ NMR spectra of reaction mixtures show that **8g**[OTf] is the exclusive product from the addition of a solution of Me_2PCl (0.016 mL, 0.202 mmol) and Me_3-

Table 2. Select Structural Parameters for Cyclotetraphosphinophosphonium Cations[a]

cation	P–C (Å)	P–P (Å)	C–P–C (deg)	P−P−P (deg)
8b	1.804(4) [1,1]	2.206(1) [1,2]	107.9(2) [1,1,2]	114.20(4) [2,1,5]
	1.798(3) [1,2]	2.207(1) [1,5]		101.40(4) [1,2,3]
	1.839(4) [2,3]	2.185(1) [2,3]		109.75(4) [2,3,4]
	1.857(4) [3,4]	2.197(1) [3,4]		107.92(4) [3,4,5]
	1.839(4) [4,5]	2.189(1) [4,5]		101.86(4) [4,5,1]
	1.839(4) [5,6]			
8c	1.868(2) [1,1]	2.2045(8) [1,2]	107.50(10) [1,1,5]	101.77(3) [2,1,5]
	1.816(2) [1,5]	2.1995(8) [1,5]		88.77(3) [1,2,3]
	1.836(2) [2, 11]	2.2255(8) [2,3]		90.70(3) [2,3,4]
	1.840(2) [3,17]	2.2570(8) [3,4]		102.80(3) [3,4,5]
	1.836(2) [4, 23]	2.2299(8) [4,5]		98.32(3) [1,5,4]
	1.829(2) [5,29]			
8e	1.794(3) [1,1]	2.192(1) [1,2]	106.6(1) [1,1,2]	107.87(4) [2,1,5]
	1.804(3) [1,2]	2.183(1) [1,5]		95.54(4) [1,2,3]
	1.876(3) [2,3]	2.223(1) [2,3]		104.56(4) [2,3,4]
	1.885(3) [3,9]	2.220(1) [3,4]		109.08(4) [3,4,5]
	1.862(3) [4,15]	2.202(1) [4,5]		97.46(4) [4,5,1]
	1.876(3) [5,21]			
8f	1.799(2) [1,1]	2.2221(6) [1,2]	111.59(8) [1,1,7]	107.36(2) [2,1,5]
	1.798(2) [1,7]	2.2072(6) [1,5]		96.52(2) [1,2,3]
	1.829(2) [2,13]	2.2318(6) [2,3]		93.59(2) [2,3,4]
	1.843(2) [3,19]	2.2392(6) [3,4]		89.56(2) [3,4,5]
	1.842(2) [4,25]	2.2251(6) [4,5]		91.64(2) [4,5,1]
	1.827(2) [5,31]			
8g	1.790(2) [1,1]	2.1864(9) [1,2]	107.9(1) [1,1,2]	102.79(4) [2,1,5]
	1.797(2) [1,2]	2.1845(9) [1,5]		91.91(3) [1,2,3]
	1.830(2) [2,3]	2.2187(9) [2,3]		96.78(3) [2,3,4]
	1.827(2) [3,9]	2.2242(9) [3,4]		108.47(3) [3,4,5]
	1.843(2) [4,15]	2.2115(9) [4,5]		96.41(4) [1,5,4]
	1.830(2) [5,21]			

[a] Numbers in square brackets correspond to atom labels shown in Figure 1.

Table 3. $^{31}P\{^1H\}$ NMR Parameters for the ABCDX Spin System of **8a**[OTf] and **8c**[$GaCl_4$][a]

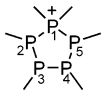

cation	[$(PhP)_4PPhMe$]$^+$ **8a**[OTf]	[$(PhP)_4PPh^tBu$]$^+$ **8c**[$GaCl_4$]
figure	2	4
δ (ppm)	22 [1]	26.5 [1]
	−25 [2]	−28.5 [2]
	−32 [3]	−45.9 [3]
	−34 [4]	−38.4 [4]
	−36 [5]	−34.1 [5]
$^1J_{PP}$ (Hz)	−315 [1,2]	−404 [1,2]
	−328 [1,5]	−350 [1,5]
	−193 [2,3]	−137 [2,3]
	−166 [3,4]	−178 [3,4]
	−162 [4,5]	−229 [4,5]
$^2J_{PP}$ (Hz)	17 [1,3]	38 [1,3]
	30 [1,4]	6 [1,4]
	58 [2,4]	66 [2,4]
	−15 [2,5]	−19 [2,5]
	71 [3,5]	4 [3,5]

[a] Numbers in square brackets correspond to the atom numbering scheme shown. The framework is depicted as planar as the simulated data provides information of the connectivity and symmetry of the phosphorus framework but not the stereochemistry.

SiOTf (0.046 mL, 0.254 mmol) in CH_2Cl_2 (4 mL) to solid $(PhP)_4$ (0.087 g, 0.202 mmol).

Results and Discussion

A series of cyclotetraphosphinophosphonium **8** salts have been prepared from cyclopolyphosphines by means of five reaction types, as illustrated in Scheme 2. Reactions of cyclopentaphosphines **4a** (in C_6H_6) or **4b** (in CH_2Cl_2) with MeOTf occur rapidly at room temperature to give **8a**[OTf] and **8b**[OTf] (Scheme 2a), respectively. Interestingly, mixtures of cyclotetraphosphine **3a** and MeOTf also show essentially quantitative formation of **8a**[OTf] (Scheme 2b), contrasting previous observations concerning the formation of cyclotriphosphinophosphonium **7** cations from methylation of $(CyP)_4$ (**3c**).[7] Alkylation of **4a** is also effected by a mixture of $GaCl_3$ and ^{t}BuCl according to Scheme 2c to give **8c**[$GaCl_4$].

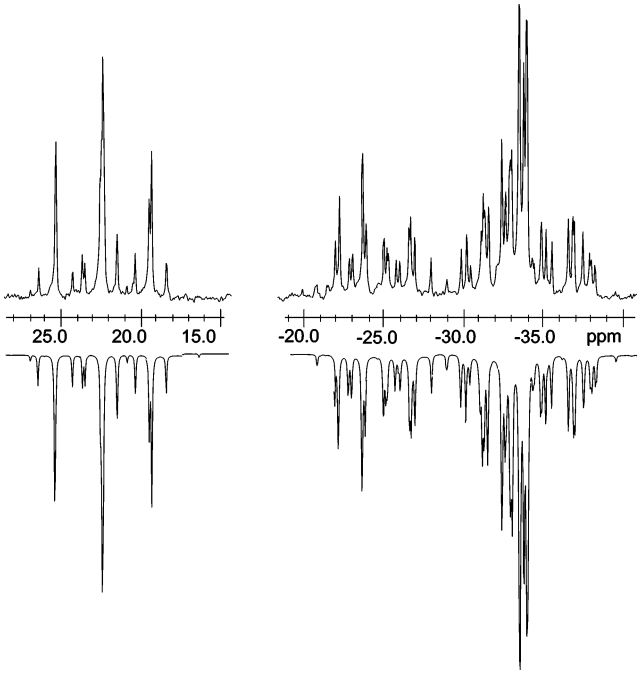

Figure 2. Experimental (top) and simulated (inverted) $^{31}P\{^1H\}$ NMR spectrum at 101.3 MHz for **8a**[OTf].

Although it has not been possible to isolate **8d**[OTf], $^{31}P\{^1H\}$ NMR spectra of reaction mixtures containing $(CyP)_4$ (**3c**), Ph_2PCl and Me_3SiOTf indicate that the reaction proceeds predominantly according to Scheme 2d. Moreover, an analogous reaction is observed for mixtures containing $(CyP)_4$ (**3c**), Me_2PCl and Me_3SiOTf, as well as for $(PhP)_4$ with Me_2PCl or Ph_2PCl and Me_3SiOTf, which shows essentially quantitative formation of **8e**−**g**[OTf]. This phosphenium ion insertion, and concurrent ring expansion process has also been observed in the formation of [$(^tBuP)_3PMe_2$][OTf] (of type **7**) from **2d** and Me_2PCl/TMSOTf.[7]

In contrast, reactions of cyclopentaphosphine $(PhP)_5$ (**4a**), Me_3SiOTf, and Me_2PCl or Ph_2PCl afford **8f**[OTf] and **8g**[OTf], respectively (Scheme 2e). In these instances, no net ring expansion is observed, emphasizing the favorability of pentaphosphorus over hexaphosphorus monocations. Consistently, **8b** is formed in the reaction mixture of $(MeP)_5$ (**4b**) with Me_3SiOTf and Me_2PCl according to Scheme 2e.

Figure 1 shows an ORTEP plot of the solid-state structure for each cation **8b**, **8c**, **8e**, **8f**, and **8g**, as well as an "in-plane" view of the phosphorus framework showing only the α-carbon centers. A summary of crystallographic data is listed in Table 1 and selected structural parameters for the cations are presented in Table 2. Crystallographic data was also obtained for **8a**[OTf], but due to severe disorder in the crystals, structural details excluding the assignment of configuration and connectivity, could not be determined. All crystals contain only the *R, S, S, R* (shown for each) and *S, R, R, S* isomers of the 16 possible

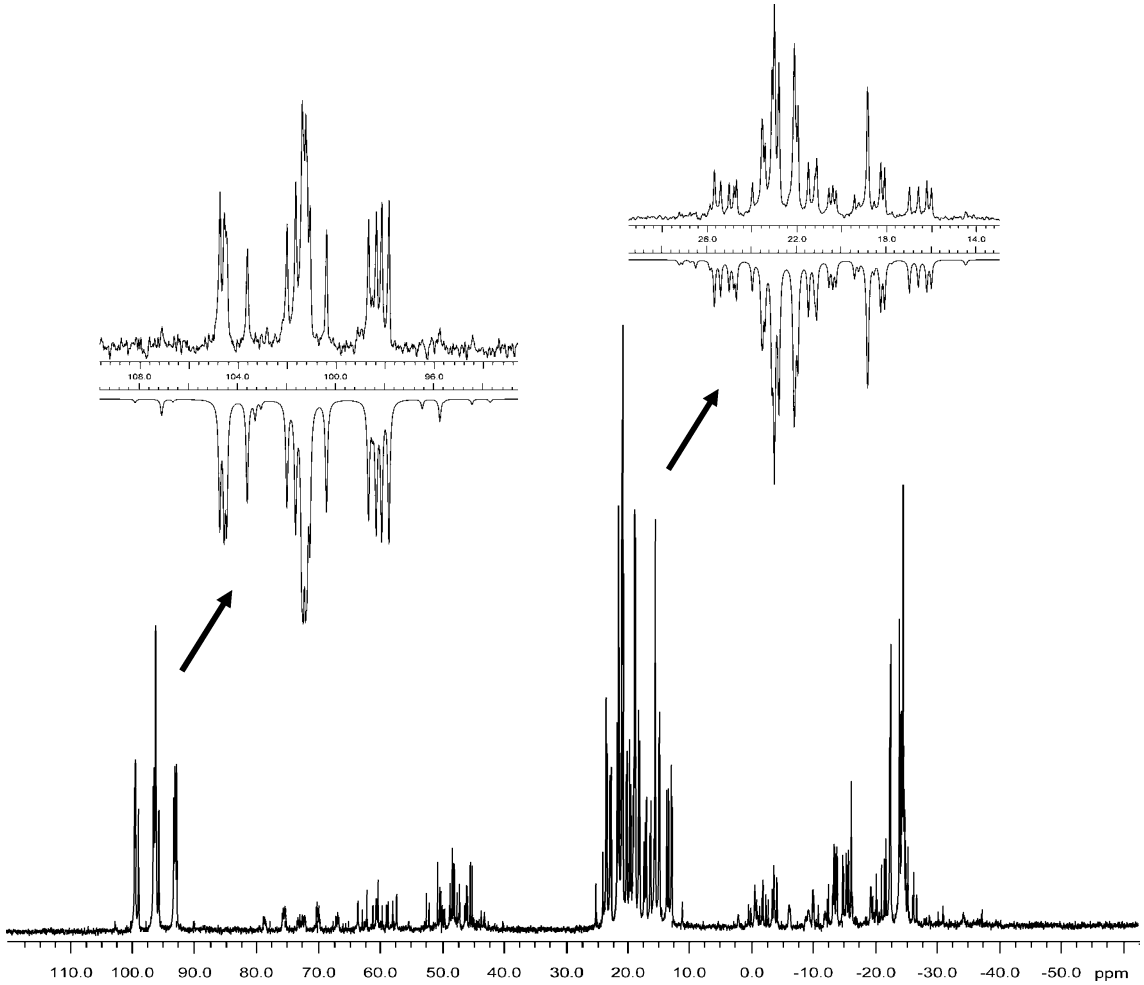

Figure 3. $^{31}P\{^{1}H\}$ NMR spectrum at 101.3 MHz for the reaction mixture containing **4b** and MeOTf, with expansions for the AA′BB′X spin system of one enantiomeric pair of **8b**[OTf] and the simulated (inverted) patterns.

Table 4. $^{31}P\{^{1}H\}$ NMR Parameters for Cyclotetraphosphinophosphonium Cations **8** Exhibiting AA′BB′X Spin Systems[a]

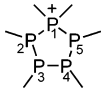

cation	$[(MeP)_4PMe_2]^+$ **8b**[b]	$[(CyP)_4PPh_2]^+$ **8d**[b]	$[(CyP)_4PMe_2]^+$ **8e**[c]	$[(PhP)_4PPh_2]^+$ **8f**[c]	$[(PhP)_4PMe_2]^+$ **8g**[c]
figure	3	5	6	7	8
$\delta_3 = \delta_4$ (ppm)	24	−15	−14	−42	−26
$\delta_2 = \delta_5$ (ppm)	20	−2	−8	−36	−32
δ_1 (ppm)	101	52	42	22	27
$^1J_{34}$ (Hz)	−263	−247	−255	−142	−186
$^1J_{32} = {}^1J_{45}$ (Hz)	−277	−262	−264	−160	−192
$^1J_{21} = {}^1J_{51}$ (Hz)	−346	−352	−332	−325	−315
$^2J_{31} = {}^2J_{41}$ (Hz)	−3	2	9	28	24
$^2J_{35} = {}^2J_{42}$ (Hz)	16	0	0	79	50
$^2J_{25}$ (Hz)	−19	−21	−21	−14	−15

[a] Subscripts on δ and J correspond to the atom numbering scheme shown. [b] CH_2Cl_2. [c] $CDCl_3$.

stereoisomers for each cation (discounting the chiral phosphonium center in **8c**). Both enantiomers of **8c**[$GaCl_4$], **8f**[OTf], and **8g**[OTf] are related by crystallographic symmetry, whereas the same pair of enantiomers in **8b** is present in the asymmetric unit and as such is not related by crystallographic symmetry. Crystals of **8e**[OTf] have two independent ions in the asymmetric unit. Table 2 presents selected structural parameters for only one (*R*, *S*, *S*, *R*) cation for each of **8b**[OTf] **8c**[$GaCl_4$], **8e**[OTf], **8f**[OTf], and **8g**[OTf].

Although the cations **8b**, **8c**, **8e**, **8f**, and **8g** adopt the most favorable all-*trans* configurations for the four phosphine centers, each derivative has a unique C_1 conformation in the solid state. As determined by the Platon program,[36] pentaphosphorus frameworks **8b**, **8f**, and **8g** are best described as adopting an envelope (E) conformation, whereas **8c** and **8e** adopt twist (T) conformations. An E conformer is defined by four coplanar atoms, whereas a T conformer is defined by the coplanarity of three atoms and the midpoint of the opposite bond. A specific

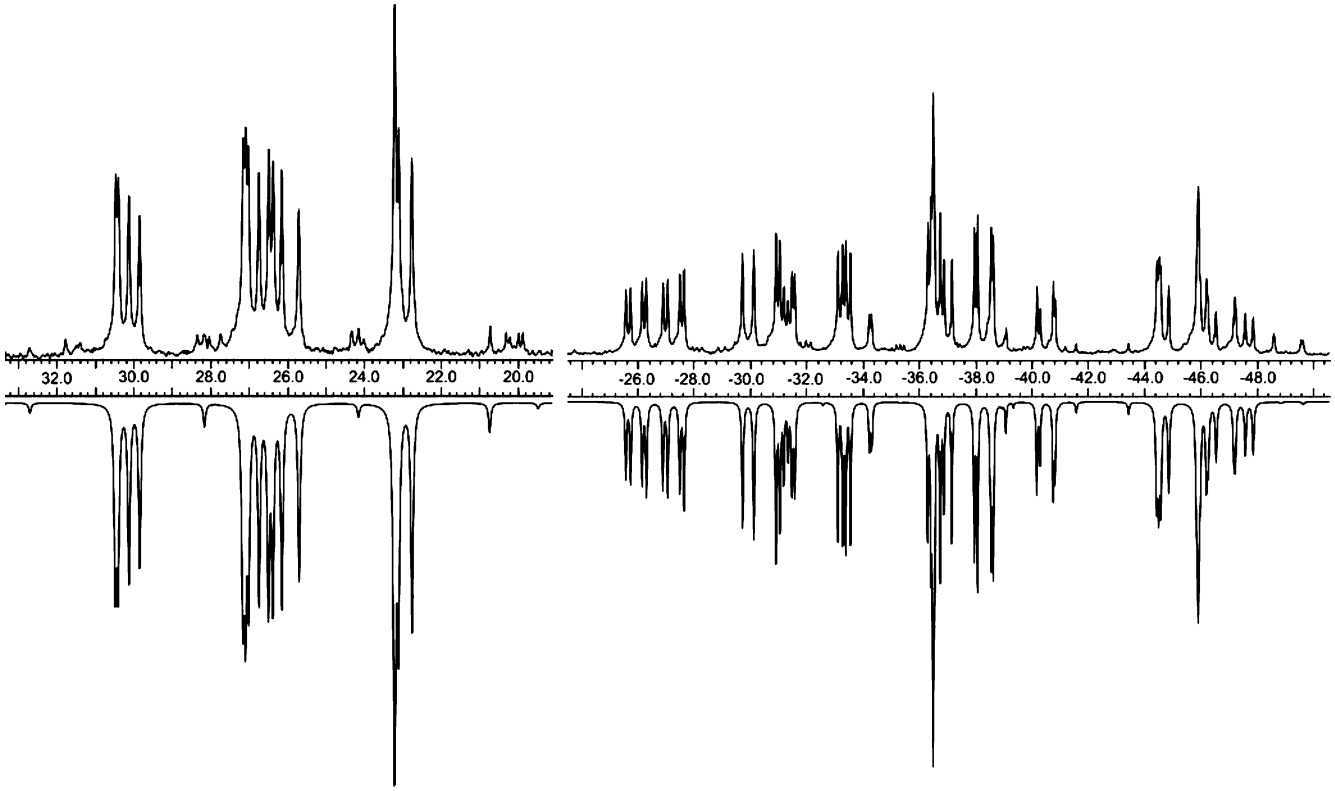

Figure 4. Experimental (top) and simulated (inverted) $^{31}P\{^{1}H\}$ NMR spectrum at 101.3 MHz for **8c**[OTf].

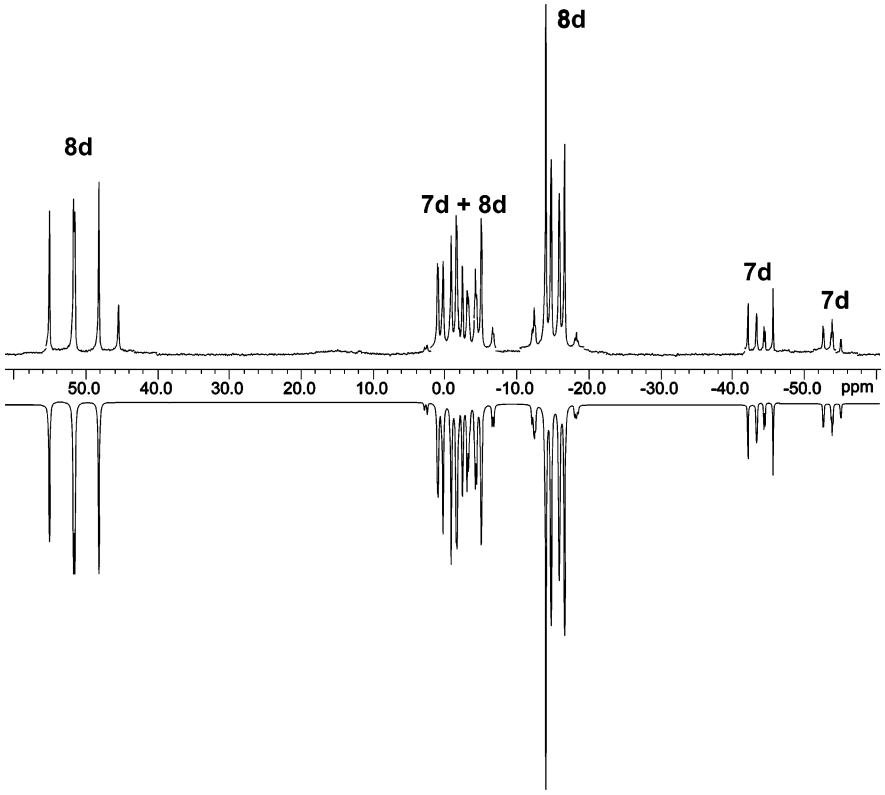

Figure 5. Experimental (top) and simulated (inverted) $^{31}P\{^{1}H\}$ NMR spectrum for the reaction mixture containing $(CyP)_4$, **3c**, Ph_2PCl and Me_3SiOTf. Signals are assigned to **8d** (enantiomeric pair) and **7d**.

E or T conformation is identified as ^{x}E, E_x, or $^{x}T_y$, where *x* and *y* refer to the numerical label of the atoms above (superscripted) and/or below (subscripted) the conformation-defining plane. For the T conformations, one (**8e**) has the phosphonium center outside of the defining plane, and in the other (**8c**), the phosphonium center is incorporated into the plane. One of the three E conformations has the phosphonium center at the fold (**8g**), and the other two are differentiated by the configuration at the apex of the envelope: axial for **8b** and equatorial for **8f**.

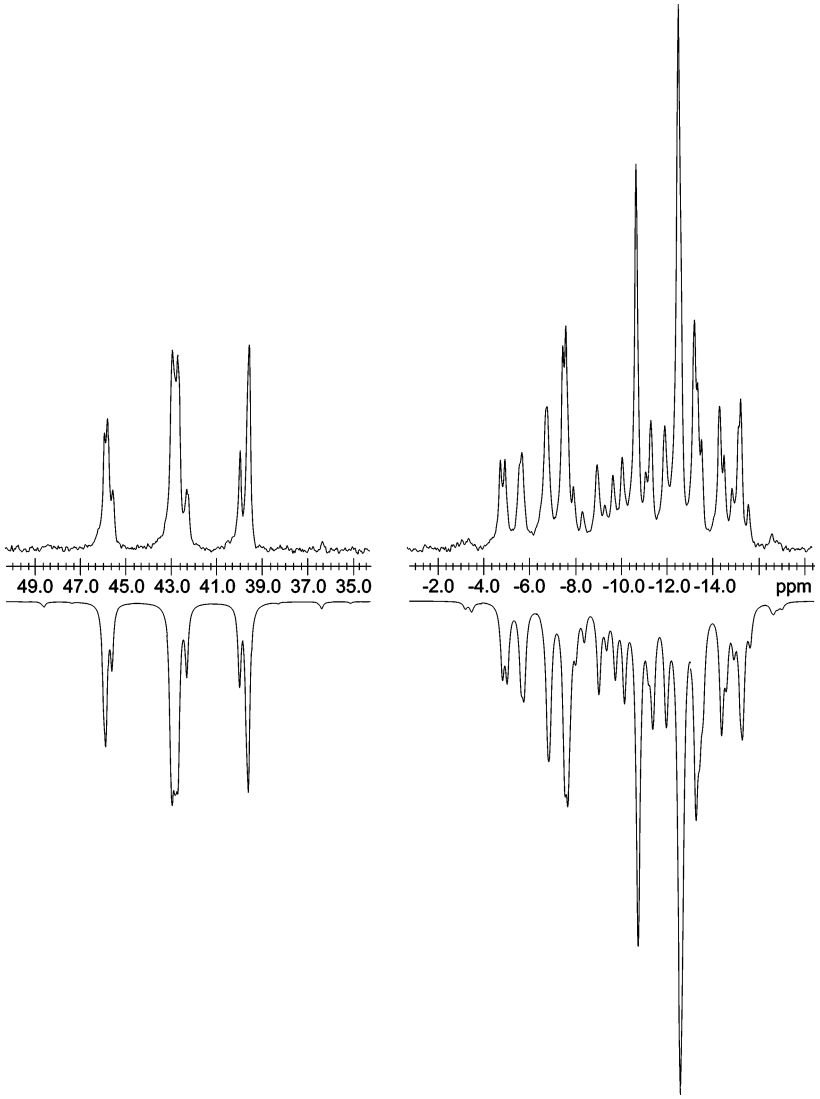

Figure 6. Experimental (top) and simulated (inverted) $^{31}P\{^{1}H\}$ NMR spectrum at 101.3 MHz for **8e**[OTf].

Iterative simulation of the experimental $^{31}P\{^{1}H\}$ NMR spectrum for redissolved crystals of **8a**[OTf] in $CDCl_3$ reveal an ABCDX spin system assigned to the enantiomeric pair **8′a** and **8″a** (Table 3, Figure 2). An ABCDX spin system is also observed upon redissolution of crystals of **8c**[$GaCl_4$] in MeCN (Table 3, Figure 4). Thus, in spite of the five stereogenic centers, only one of a possible 16 enantiomeric pairs of **8a** and **8c** are observed in solution (redissolved crystals and reaction mixtures). Therefore, alkylation of **4a** occurs selectively at either of the *cis*-configured phosphorus centers (Scheme 2a and c), as further supported by the crystallographic data for **8c**[$GaCl_4$] and **8a**[OTf]. The $^{1}J_{PP}$ coupling constants for **8a** and **8c** are consistent with the sterically favored all-*trans* arrangement of the substituents on the phosphine centers[37,38] observed in the solid state.

The AA′BB′X spin systems (Table 4) observed in the $^{31}P\{^{1}H\}$ NMR spectra of reaction mixtures corresponding to Scheme 2d and 2e are also consistent with the sterically favored all-trans configuration of substituents for the corresponding derivatives of **8**.[37,38] In the case of **8b** (Figure 3), a number of unassigned signals are observed in spectra of the reaction mixture as well as in spectra of redissolved crystalline materials. These are possibly due to the formation of other stereoisomers, consistent with similar observations for the oxidation of **4b** with oxygen.[39] We speculate that these other stereoisomers are only energetically favorable with small substituents, as even the oxidation of $(EtP)_5$ with sulfur resulted in only one enantiomeric pair of the corresponding pentaphosphorus monosulfide.[40]

The $^{31}P\{^{1}H\}$ NMR spectrum of the reaction mixture of $(CyP)_4$ (**3c**) with Ph_2PCl and Me_3SiOTf (Scheme 2c; Figure 5) indicates that **8d** is a dominant product, with a minor component that is simulated with an AB_2X spin system assigned to the cyclic tetraphosphorus monocation $[(CyP)_3PPh_2]$[OTf] (**7c**[OTf]). Reactions according to Scheme 2d and 2e, for the formation of **8e**, **8f** and **8g** proceed cleanly and expansions for the $^{31}P\{^{1}H\}$ NMR AA′BB′X spin systems for reaction mixtures are shown in Figure 6, 7, and 8, respectively.

The AA′BB′X spin system observed in the $^{31}P\{^{1}H\}$ NMR spectra for derivatives of **8**[OTf] (excluding **8a** and **8c**) imply high molecular symmetry in solution that is inconsistent with

(36) Spek, A. L. *J. Appl. Crystallogr.* **2003**, *36*, 7−13.
(37) Albrand, J. P.; Robert, J. B. *C. R. Acad. Sci. Paris* **1978**, *C287*, 89−91.
(38) Albrand, J. P.; Robert, J. B. *Chem. Commun.* **1974**, 644−645.
(39) Baudler, M.; Koch, P.; Hasenbach, J.; Hahn, J. *Z. Anorg. Allg. Chem.* **1989**, *576*, 17−24.
(40) Baudler, M.; Koch, P. *Z. Naturforsch.* **1989**, *44b*, 1167−1170.

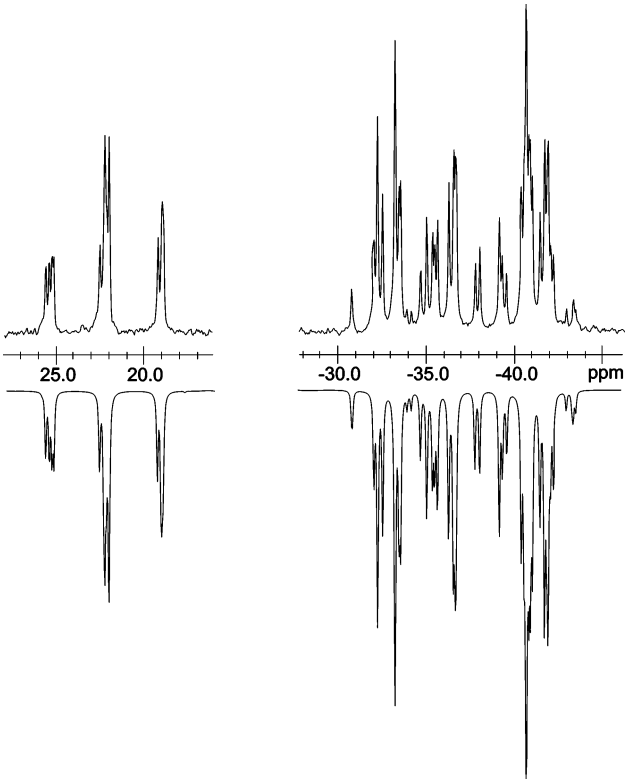

Figure 7. Experimental (top) and simulated (inverted) $^{31}P\{^{1}H\}$ NMR spectrum at 101.3 MHz for **8f**[OTf].

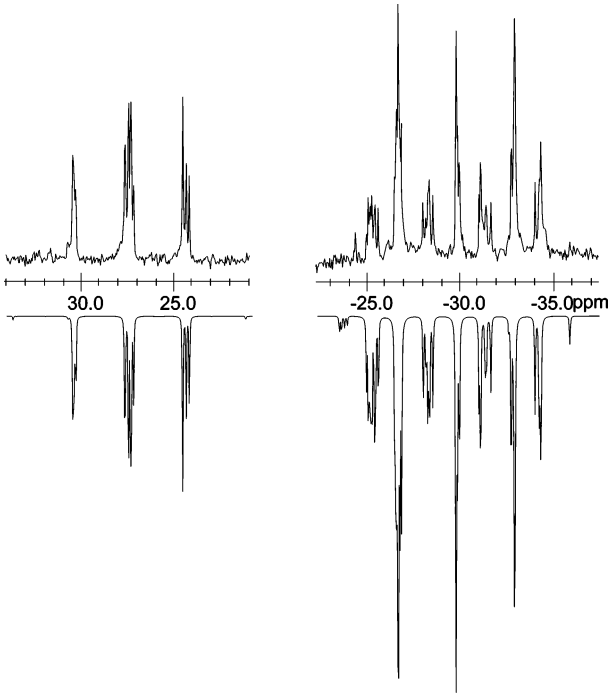

Figure 8. Experimental (top) and simulated (inverted) $^{31}P\{^{1}H\}$ NMR spectrum at 101.3 MHz for **8g**[OTf].

the C_1 solid-state symmetry observed for structures **8b**, **8c**, **8e**, **8f**, and **8g**. A number of previously reported five-membered rings with catenated, or partially catenated phosphorus frameworks also adopt low symmetry (C_1) structures in the solid state (**9**,[41,42] **10**,[43] **11**,[44] **12**,[45] **13a**,[46] **13b**[47]), whereas NMR spectroscopic data indicate higher symmetry in solution (**9**,[38] **10**,[48,49] **11**,[44] **12**,[45] **13a**,[46] **13b**[47]). Inversion at phosphorus (made possible by relatively low barriers in catenated systems),[50] static C_2 twist or C_s envelope conformations, and pseudorotation have all been suggested to rationalize these observations.

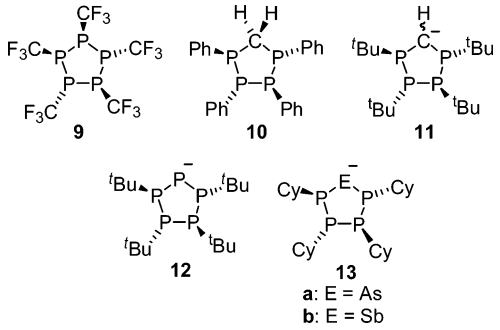

The observation of an ABCDX spin system for **8a**[OTf] and **8c**[$GaCl_4$] implies that inversion at phosphorus is slow on the NMR time scale. This is consistent with the previous conclusion that inversion likely occurs at the anionic carbon in **11**,[44] as opposed to the phosphine centers, although rapid inversion at phosphorus could not be definitively excluded. In the present case, the observed ABCDX spin systems make it unreasonable to invoke rapid inversion at phosphorus to rationalize the symmetry of monocations **8** in solution. This also signifies that the AA′BB′X spin systems must result from effective C_2, rather than C_s, symmetry.

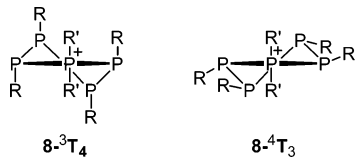

The observation of five unique solid state C_1 structures for derivatives **8b**, **8c**, **8e**, **8f**, and **8g** contradicts the idea of static twist conformations of C_2 symmetry (**8**-$^{3}T_4$, **8**-$^{4}T_3$) in solution, initially proposed for **10**.[49,51] We therefore interpret the contrasting solid state and solution symmetry for cyclotetraphosphinophosphonium cations in terms of a pseudorotation in solution, as previously proposed for **9**.[38] This low-energy ring puckering process gives rise to a conformational exchange without inversion at any nucleus and is well-known in organic ring systems.[52,53] Figure 9 presents the E and T conformations of all-*trans* substituted cyclotetraphosphinophosphonium cations as a function of the phase angle of pseudorotation (φ).[54] Of the

(41) Spencer, C. J.; Simpson, P. G.; Lipscomb, W. N. *Acta Cryst.* **1962**, *15*, 509.
(42) Spencer, C. J.; Lipscomb, W. N. *Acta Cryst.* **1961**, *14*, 250−256.
(43) Lex, J.; Baudler, M. *Z. Anorg. Allg. Chem.* **1977**, *431*, 49−60.
(44) Wolf, R.; Hey-Hawkins, E. *Chem. Commun.* **2004**, 2626−2627.
(45) Schisler, A.; Lonnecke, P.; Huniar, U.; Ahlrichs, R.; Hey-Hawkins, E. *Angew. Chem., Int. Ed.* **2001**, *40*, 4217−4219.
(46) Bashall, A.; García, F.; Hopkins, A. A.; Wood, J. A.; McPartlin, M.; Woods, A. D.; Wright, D. S. *Dalton Trans.* **2003**, 1143−1147.
(47) Bashall, A.; Beswick, M. A.; Choi, N.; Hopkins, A. D.; Kidd, S. J.; Lawson, Y. G.; Mosquera, M. E. G.; McPartlin, M.; Raithby, P. R.; Wheatley, A. A. E. H.; Wood, J. A.; Wright, D. S. *J. Chem. Soc., Dalton Trans.* **2000**, 479−486.
(48) Baudler, M.; Vesper, J.; Kloth, B.; Koch, D.; Sandmann, H. *Z. Anorg. Allg. Chem.* **1977**, *431*, 39−48.
(49) Hoffman, P. R.; Caulton, K. G. *Inorg. Chem.* **1975**, *14*, 1997−1999.
(50) Lambert, J. B.; Jackson, G. F., III; Mueller, D. C. *J. Am. Chem. Soc.* **1970**, *92*, 3093−3097.
(51) Baudler, M.; Vesper, J.; Junkes, P.; Sandmann, H. *Angew. Chem., Int. Ed.* **1971**, *10*, 940.
(52) Kilpatrick, J. E.; Pitzer, K.; Spitzer, R. *J. Am. Chem. Soc.* **1947**, *69*, 2483−2488.
(53) Strauss, H. L. *Ann. Rev. Phys. Chem.* **1983**, *34*, 301−328.

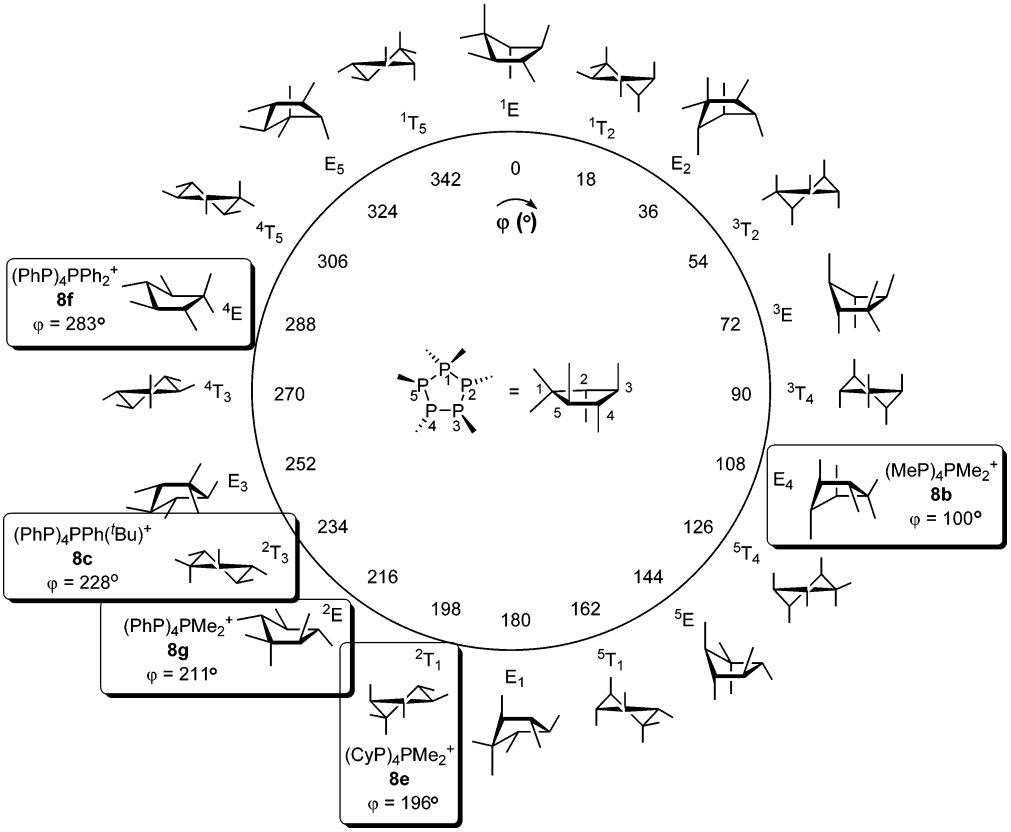

Figure 9. Graphical representation of the conformations of all-*trans* substituted cyclotetraphosphinophosphonium cations as a function of the phase angle of pseudorotation (φ, inside circle), evolved from models developed for the furanose ring.[55] The best representations of the crystallographically characterized cations are highlighted in the boxes. Envelope (E) or twist (T) conformations are labeled outside of the circle, where an envelope is defined by four coplanar atoms, and a twist by the coplanarity of three atoms and the midpoint of the opposite bond. The superscripts and subscripts in the conformation labels represent the numbered phosphorus atom above and below the plane, respectively.

20 possible conformations shown, only 11 are unique (five envelopes and six chairs), with all but $^4T_3$ and $^3T_4$ belonging to an equivalent pair related by $180 - \varphi$ (equivalent to the change in numbering sense). Values of the phase angle and the best conformational description of the ring in **8b**, **8c**, **8e**, **8f**, and **8g** were found using the Platon software[36] and are highlighted in boxes within the figure. Thus, the five unique conformations presented on the right side of Figure 8 can be seen as representing solid-state snapshots of different molecular conformations within the dynamic pseudorotation process in solution.

Though pseudorotation need not encompass all possible conformations (i.e., values of φ),[55] the pseudorotation pathway for each cyclotetraphosphinophosphonium ion must result in a time-averaged conformation where the symmetry is governed by the substitution pattern (configuration and type of specific substituent). Therefore, the spin systems observed in solution can be derived by considering the P_5 framework of each cation to be planar. This successfully colligates the AA′BB′X spin systems observed for **8b**, **8e**, **8f**, and **8g** (averaged C_2 symmetry) with their asymmetric solid-state structures and accounts for the ABCDX spin systems observed for the asymmetrically substituted derivatives **8a** and **8c**.

Summary

The first derivatives of cyclotetraphosphinophosponium cations have been isolated and represent a new series of monocyclic *catena*-phosphorus monocations. They can be prepared by the insertion of phosphenium ions (Ph_2P^+ or Me_2P^+), generated *in situ* from R_2PCl and Me_3SiOTf, into the P−P bonds of derivatives of cyclotetraphosphines **3**, or cyclopentaphosphines **4**, or by methylation of derivatives of **3a** or **4**. The reactions also demonstrated that 5-membered monocations are formed preferentially (over tetra- or hexaphosphorus alternatives) when phenyl or methyl substituents are involved at the phosphine sites. Solid-state structures reveal all-*trans* substituted phosphine centers of *R, S, S, R* and *S, R, R, S* stereochemistry and unique C_1 envelope or twist conformations. The effective C_2 symmetry observed in the $^{31}P\{^1H\}$ NMR AA′BB′X spin systems of **8** indicates that derivatives of **8**, and likely other related *catena*-phosphorus systems within five-membered rings, undergo rapid pseudorotation in solution.

Acknowledgment. NSERC and the CRC program for funding.

Supporting Information Available: X-ray crystallographic data, in CIF format for **8b**[OTf], **8f**[OTf], and **8g**[OTf]. This material is available free of charge via the Internet at http://pubs.acs.org. These files have also been deposited with the Cambridge Crystallographic Data Centre; see Table 1 for the CCDC deposition numbers.

JA070764F

(54) Cremer, D.; Pople, J. A. *J. Am. Chem. Soc.* **1975**, *97*, 1354−1358.
(55) Altona, C.; Sundaralingam, M. *J. Am. Chem. Soc.* **1972**, *94*, 8205−8212.